

Comprehensive nucleosome interactome screen establishes fundamental principles of nucleosome binding

Aleksandra Skrajna, Dennis Goldfarb, Katarzyna M Kedziora, Emily M Cousins, Gavin D Grant, Cathy J Spangler, Emily H Barbour, Xiaokang Yan, Nathaniel A Hathaway, Nicholas G Brown, Jeanette G Cook, Michael B Major, Robert K McGinty 

Nucleic Acids Research, Volume 48, Issue 17, 25 September 2020, Pages 9415–9432,

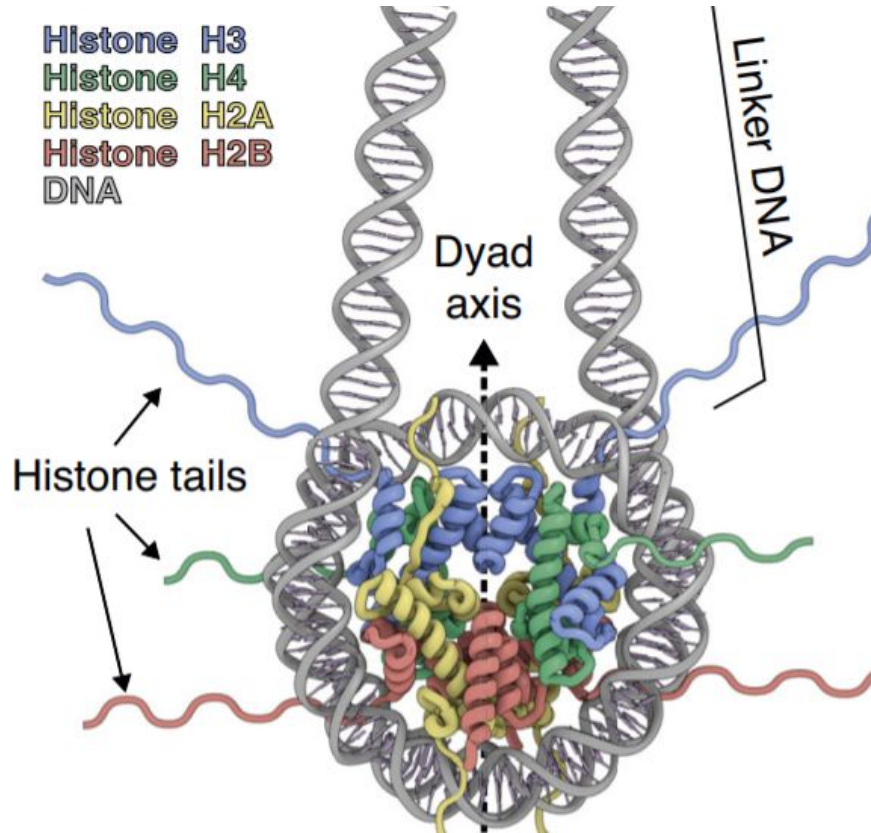
<https://doi.org/10.1093/nar/gkaa544>

Published: 07 July 2020 **Article history** ▼

Abstract

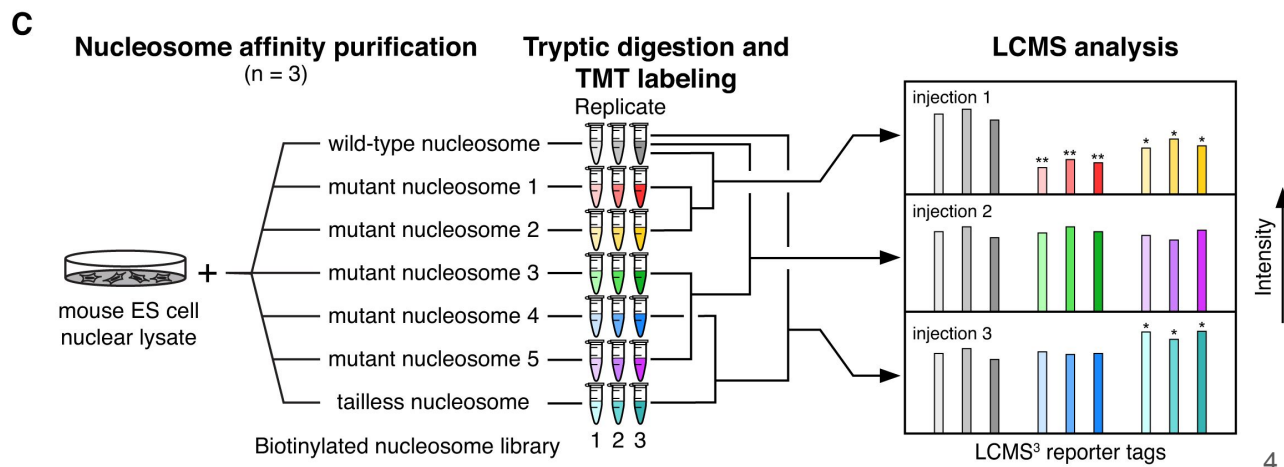
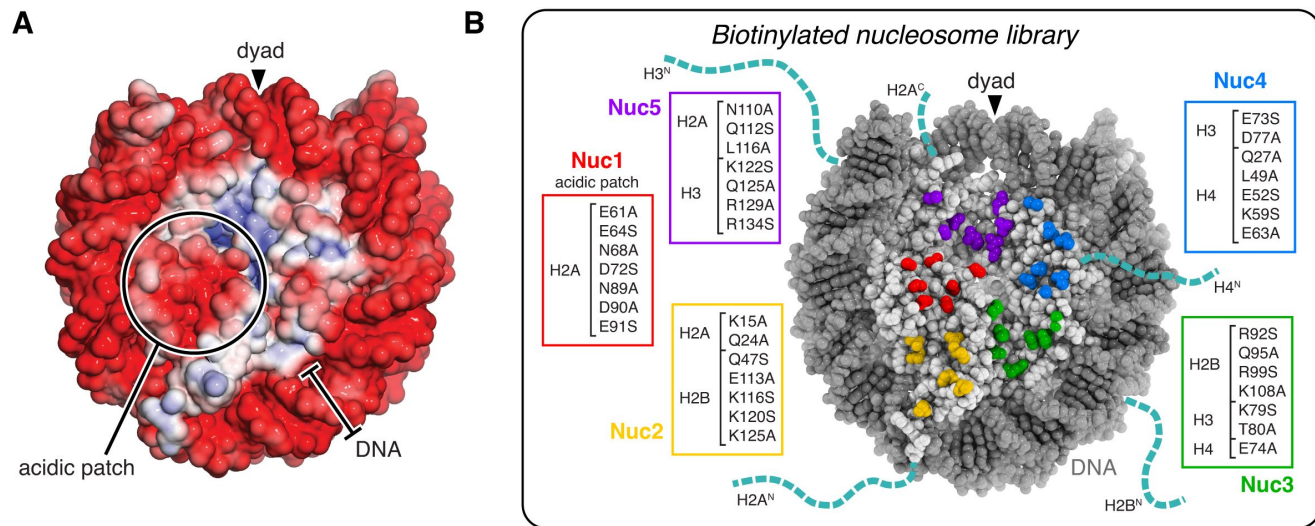
Nuclear proteins bind chromatin to execute and regulate genome-templated processes. While studies of individual nucleosome interactions have suggested that an acidic patch on the nucleosome disk may be a common site for recruitment to chromatin, the pervasiveness of acidic patch binding and whether other nucleosome binding hot-spots exist remain unclear. Here, we use nucleosome affinity proteomics with a library of nucleosomes that disrupts all exposed histone surfaces to comprehensively assess how proteins recognize nucleosomes. We find that the acidic patch and two adjacent surfaces are the primary hot-spots for nucleosome disk interactions, whereas nearly half of the nucleosome disk participates only minimally in protein binding. Our screen defines nucleosome surface requirements of nearly 300 nucleosome interacting proteins implicated in diverse nuclear processes including transcription, DNA damage repair, cell cycle regulation and nuclear architecture. Building from our screen, we demonstrate that the Anaphase-Promoting Complex/Cyclosome directly engages the acidic patch, and we elucidate a redundant mechanism of acidic patch binding by nuclear pore protein ELYS. Overall, our interactome screen illuminates a highly competitive nucleosome binding hub and establishes universal principles of nucleosome recognition.

The nucleosome

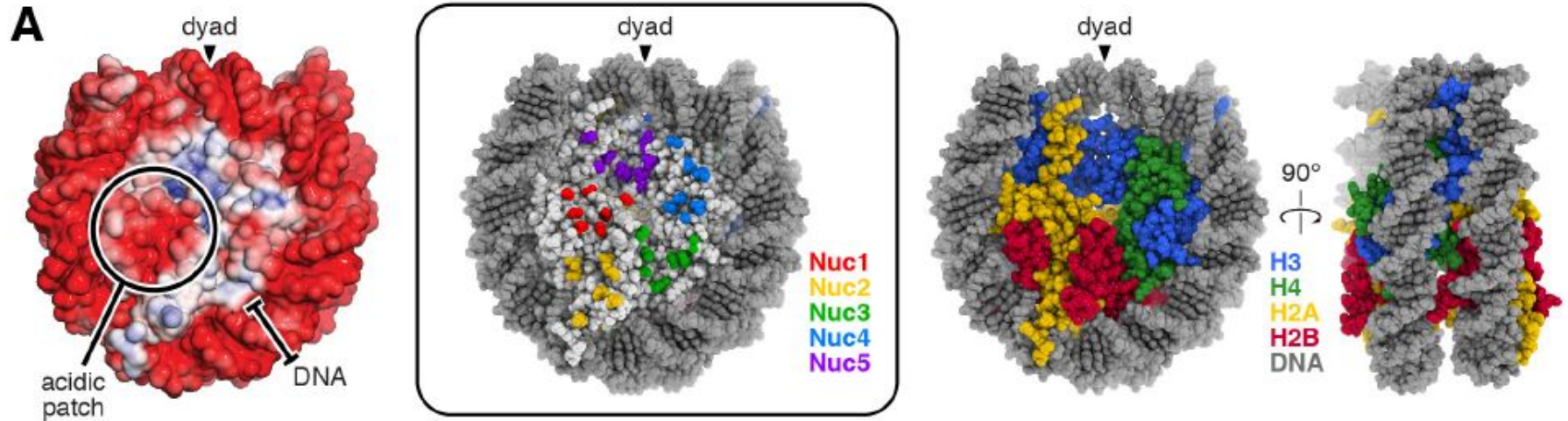


Scheme of experiments

Nucleosome affinity proteomics. **(A)** Electrostatic surface of nucleosome generated with ABPS (PDBID: 3LZ0). **(B)** Biotinylated nucleosome library showing disk mutant patches and histone tails truncated to make the tailless nucleosome. **(C)** Nucleosome affinity proteomics workflow.



Nucleosome library design and preparation

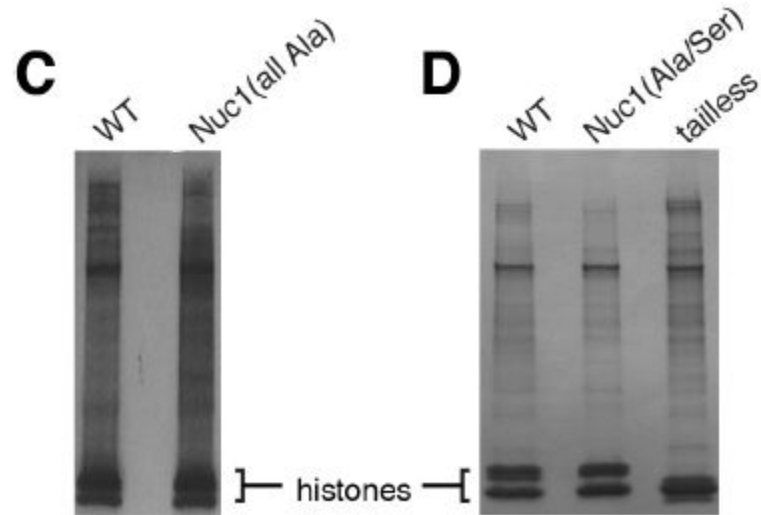


Nucleosome library and nucleosome affinity purification. (A) Nucleosome views: electrostatic (left, generated with APBS), colored by mutant disk patches (middle), and colored by histones (right, two orthogonal views).

Mutation rules

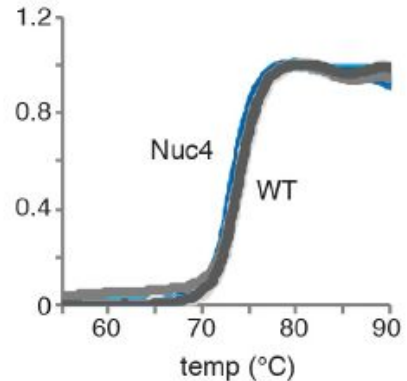
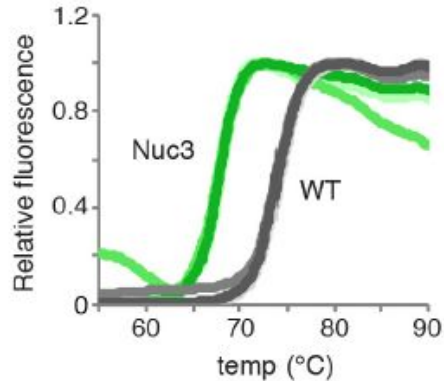
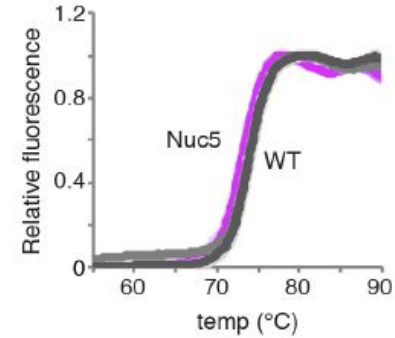
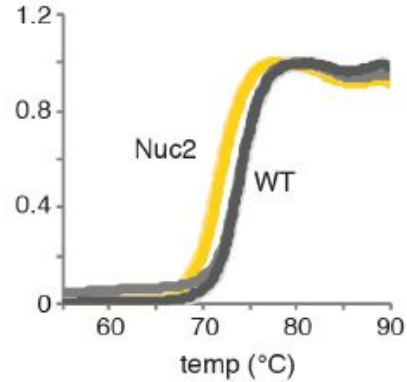
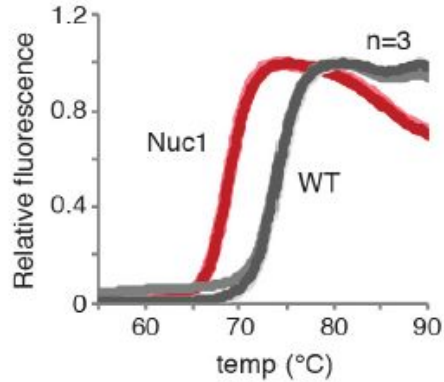
- the mutations would collectively disrupt the entire histone disk surface allowing comprehensive identification of nucleosome binding hot-spots;
- mutations would be restricted to surface-exposed side chains that are not anticipated to contribute substantially to nucleosome structure or stability;
- residues selected would be significantly chemically altered by mutation to alanine or serine (e.g. Lys, Arg, Glu, Asp, Gln, Asn);
- mutated residues would be equally distributed across a similar sized patch and
- each set of mutations would be similar in degree based on the number of atoms, hydrogen bond donors and acceptors, and charged groups removed, allowing qualitative comparison of the relative contribution of each patch to nucleosome binding.
-

Nucleosome affinity purification



(C) and (D) Representative nucleosome affinity purification assays run on 4-20% gradient gels showing increased and decreased nuclear protein binding to the acidic patch neutralized mutant nucleosomes with only alanine mutations (C), or a mix of alanine and serine mutations (D), respectively. Panel D also shows increased binding to the tailless nucleosomes.

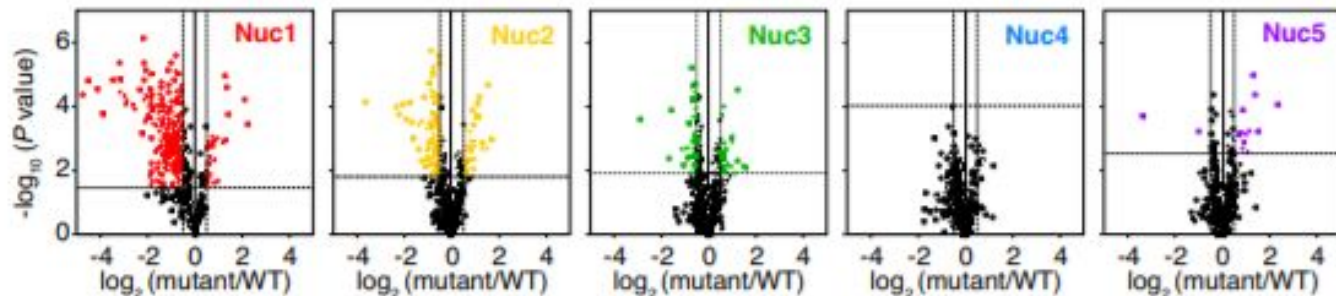
Nucleosome thermal stability



(E) Thermostability [assay](#) measuring nucleosome unfolding using SYPRO Orange fluorescence change at increasing temperatures.

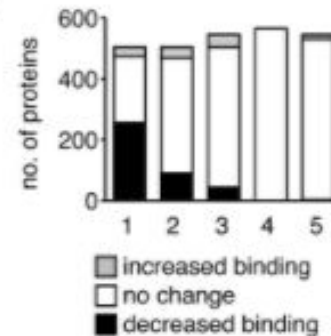
Nucleosome interactome screen

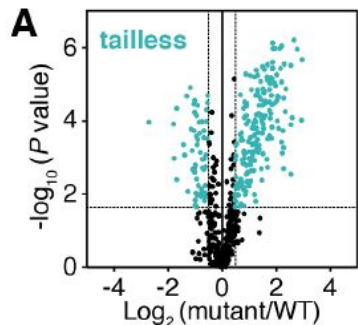
A



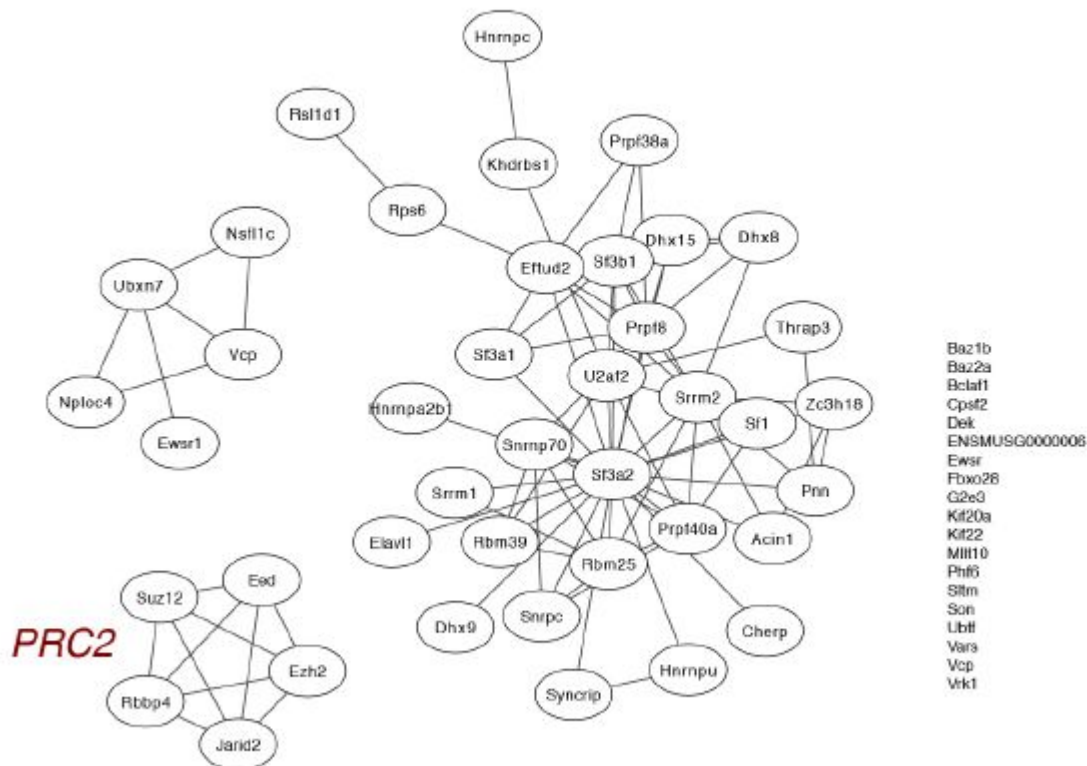
(A) Volcano plots for nucleosome binding changes in each disk patch mutant nucleosome relative to WT nucleosomes. Horizontal and vertical lines designate 5% FDR and 1.4-fold change significance thresholds, respectively. (B) Histogram illustrating number of proteins with significantly increased or decreased binding to indicated nucleosomes.

B





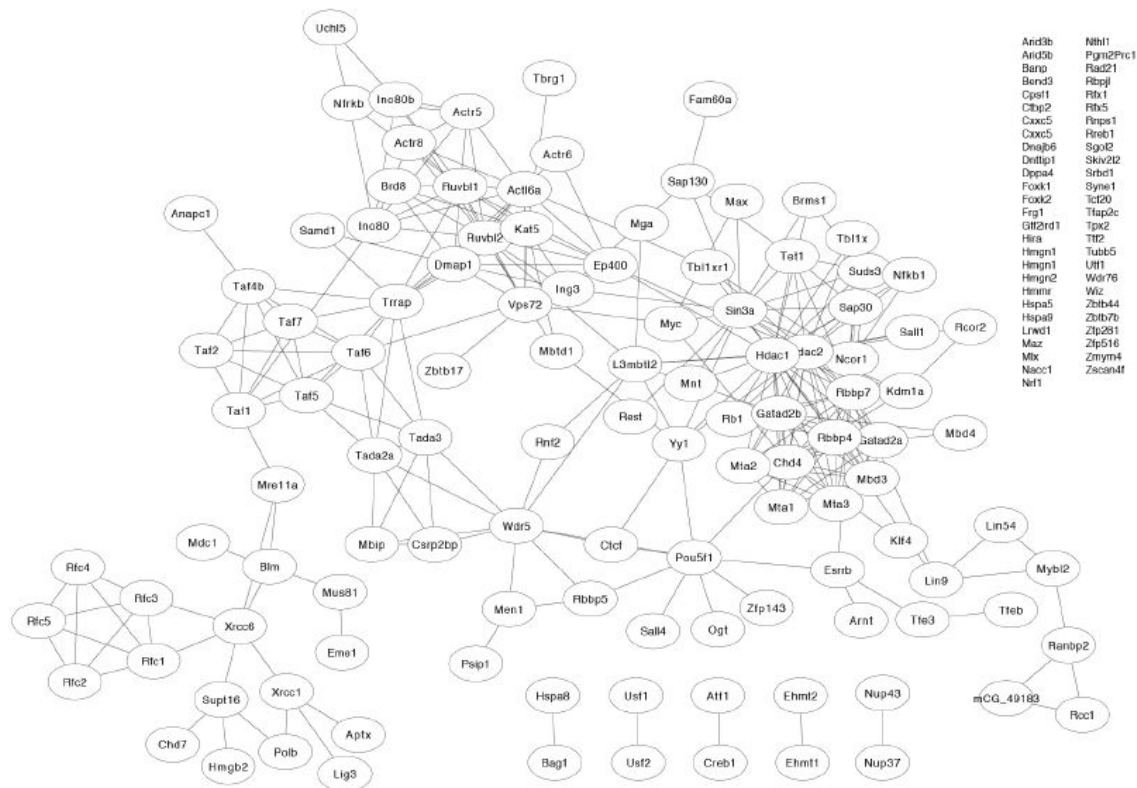
Decreased binding to tailless nucleosome



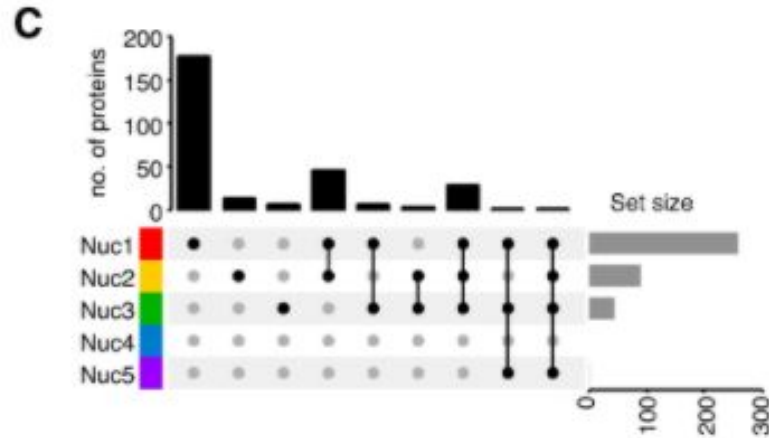
(C) and (D) Network of proteins with experimentally-established interactions with (C) decreased binding or (D) increased binding to tailless nucleosomes. Networks created using STRING v11 and plotted with Cytoscape v3.7.

(C) and (D) Network of proteins with experimentally-established interactions with (C) decreased binding or (D) increased binding to tailless nucleosomes. Networks created using STRING v11 and plotted with Cytoscape v3.7.

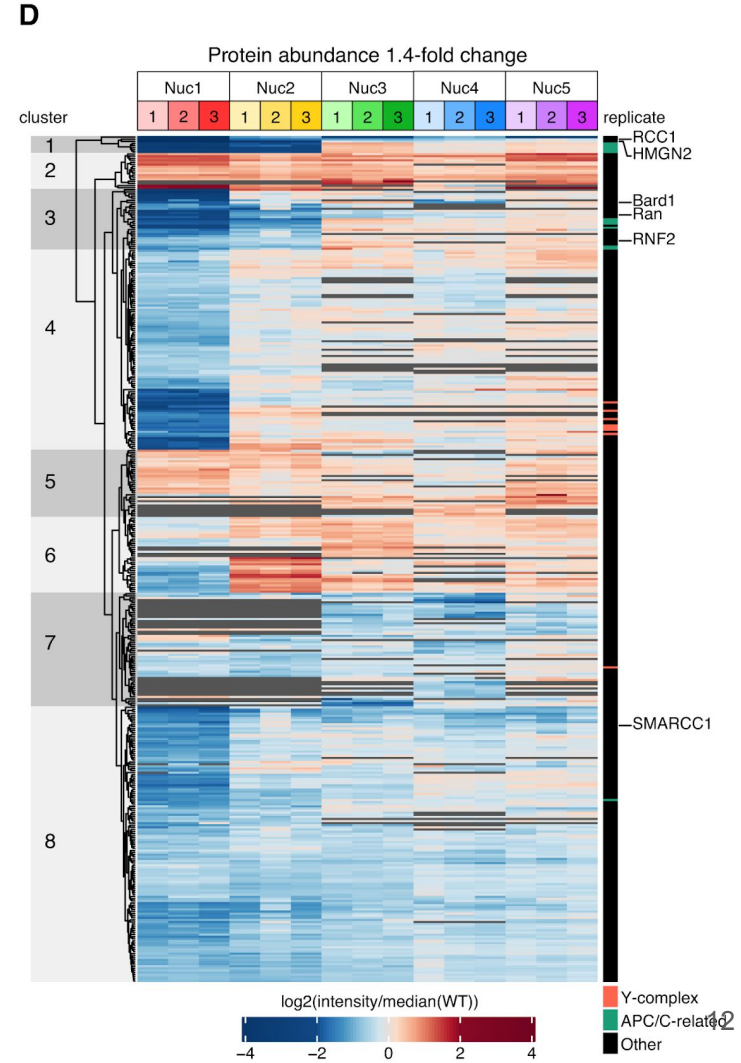
D Increased binding to tailless nucleosome



Hot-spots for nucleosome disk binding

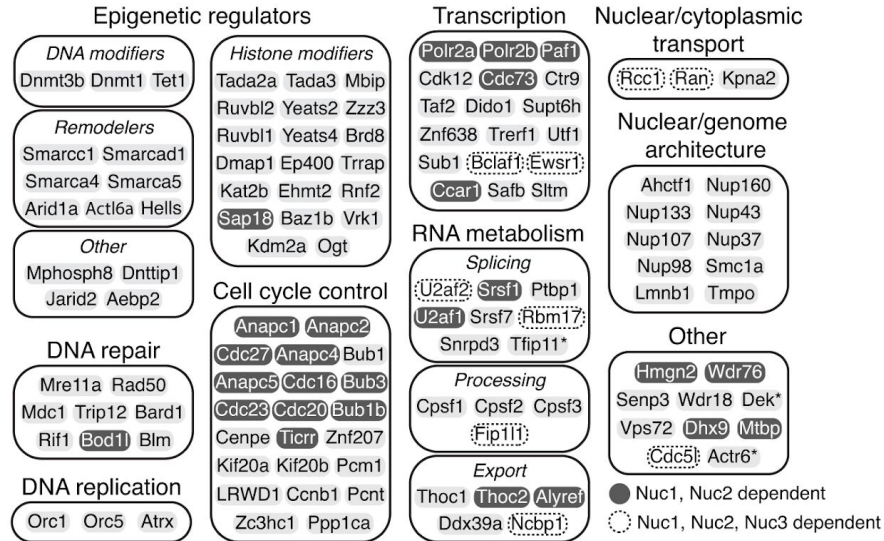


(C) Upset plot showing number of proteins with significant decreases in subset of nucleosome pulldowns, marked below.
 (D) Heat map of all significantly changed proteins, independently clustered.



Acidic patch-dependent nucleosome binding proteins

E



expected: NuA4 histone acetyltransferase (HAT) complex components TADA3 and TADA2A, ATAC HAT complex subunit DMAP1, and nuclear pore Y-complex subunits including protein ELYS,

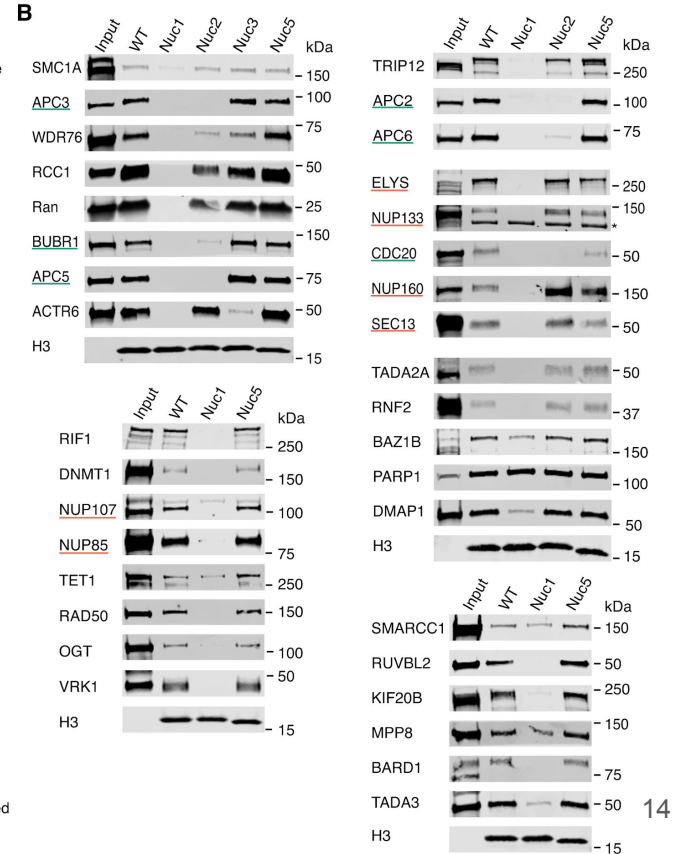
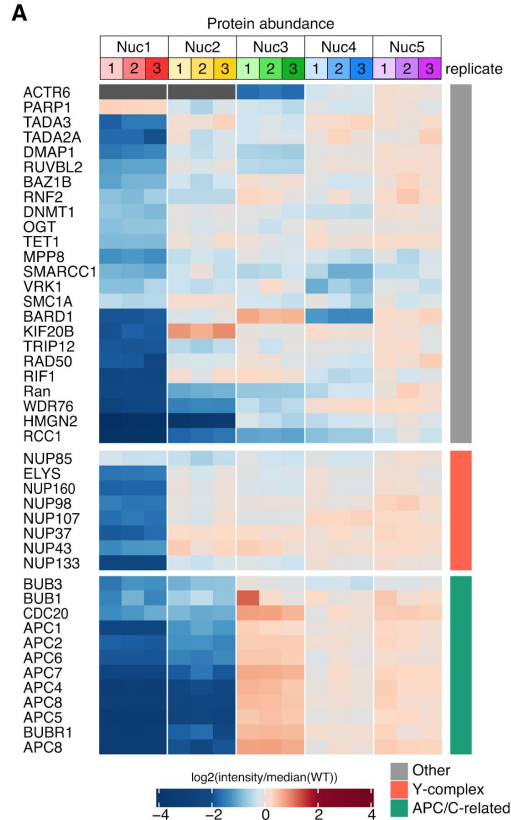
unexpected: methyllysine binding protein MPP8 and DNA double-strand break repair proteins, RIF1 and RAD50.

(E) Selected acidic patch-dependent nucleosome binding proteins.

*DEK is dependent on all but Nuc4 and Ttip11 and Actr6 are dependent on Nuc1 and Nuc3.

Nucleosome interacting proteins

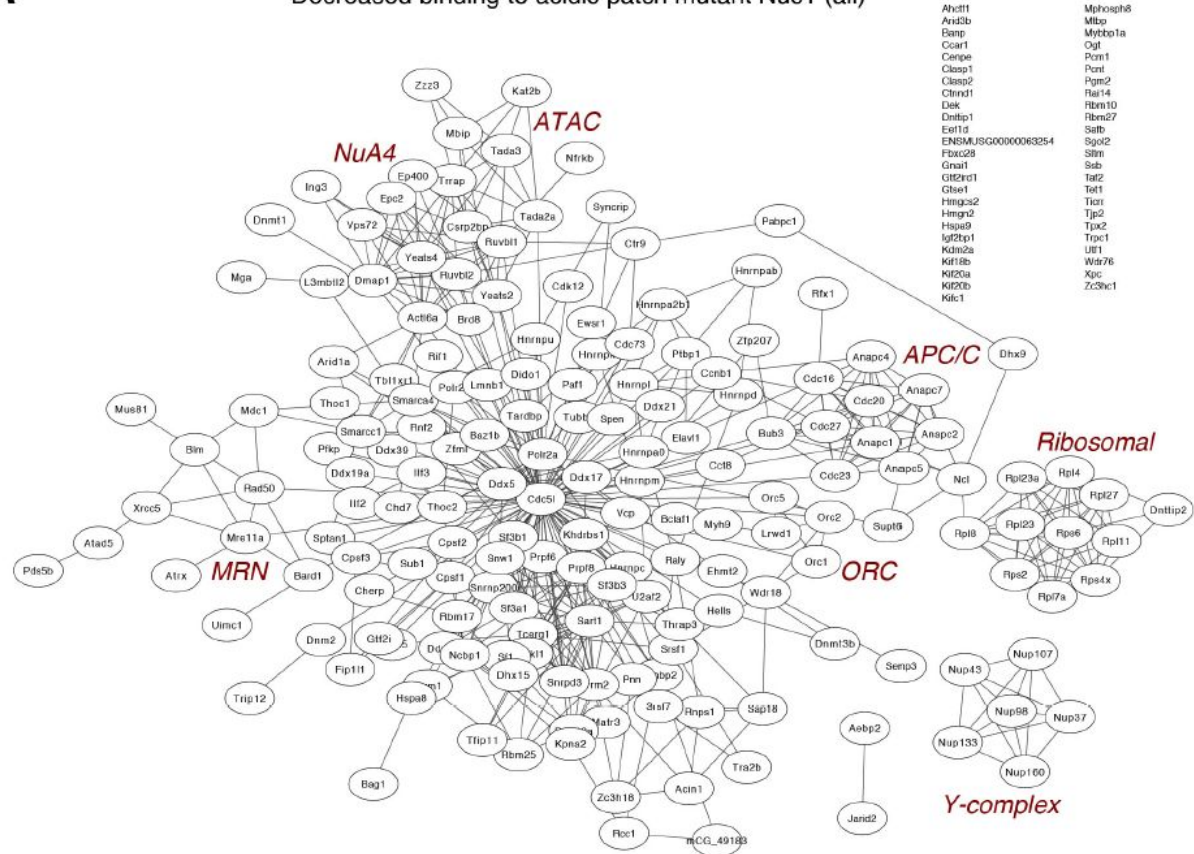
Validation of the nucleosome interactome screen. (A) Heat map as in Figure 2D of selected hits. (B) Western blots against indicated proteins following pulldown from nuclear lysate with WT or mutant nucleosomes. H3 blots demonstrate equivalent immobilized nucleosome. Underline coloring matches Y-complex and APC-related categories in panel A. Asterisk indicates non-specific band.



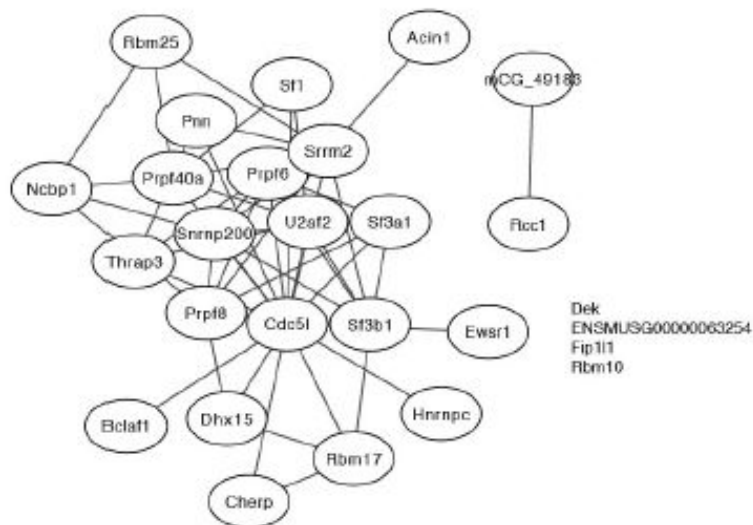
A

Decreased binding to acidic patch mutant Nuc1 (all)

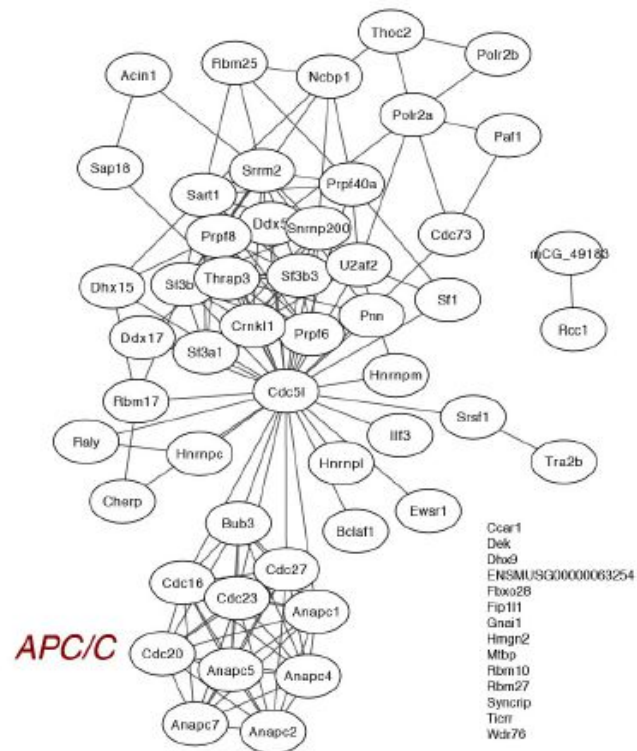
Nucleosome disk binding protein interaction networks. Experimentally established interactions of all proteins (gene names shown for brevity) with decreased binding to (A) Nuc1. Networks created using STRING v11 and plotted with Cytoscape v3.7.



C Decreased binding to Nuc1, Nuc2, and Nuc3 (all)



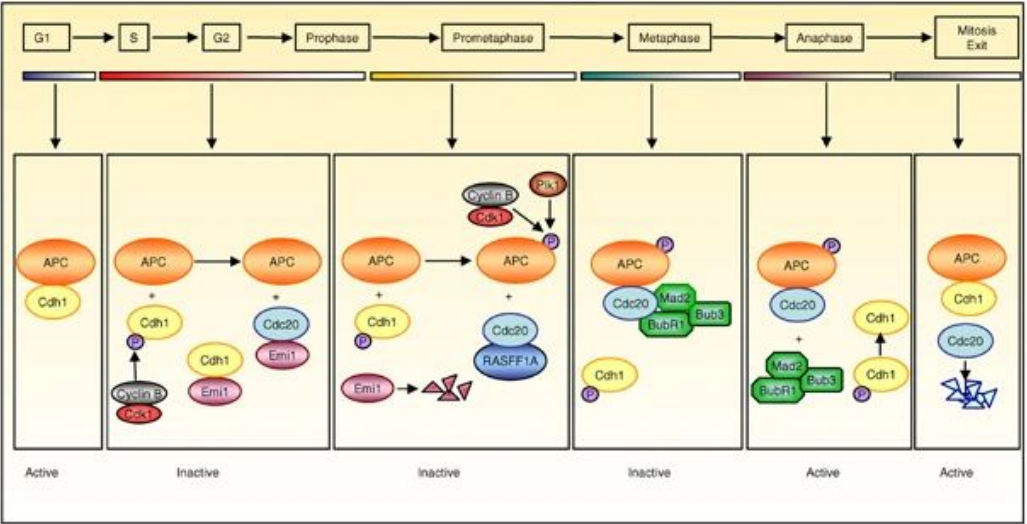
B Decreased binding to Nuc1 and Nuc2 (all)



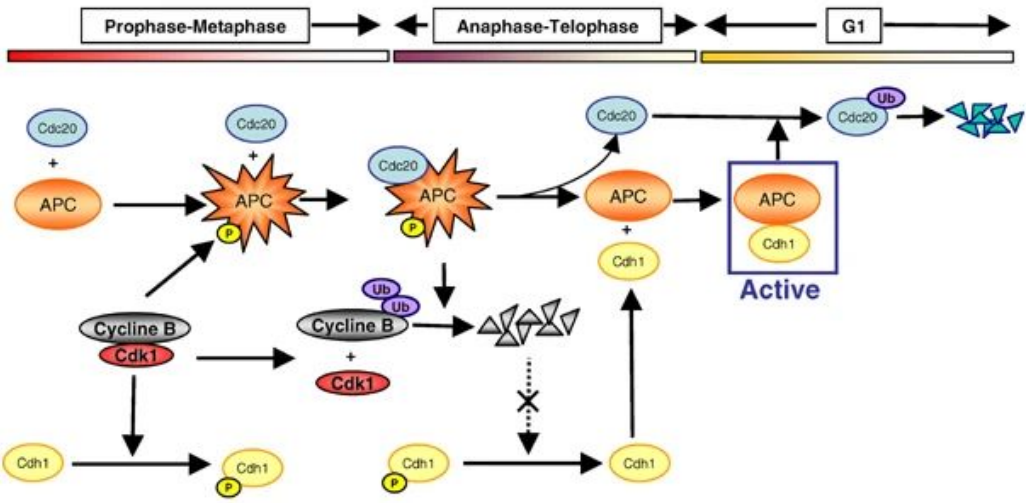
Nucleosome disk binding protein interaction networks.
Experimentally established interactions of all proteins (gene names shown for brevity) with decreased binding to
(C) Nuc1, Nuc2, and Nuc3
(B) Nuc1 and Nuc2

Networks created using STRING
v11 and plotted with Cytoscape v3.7.

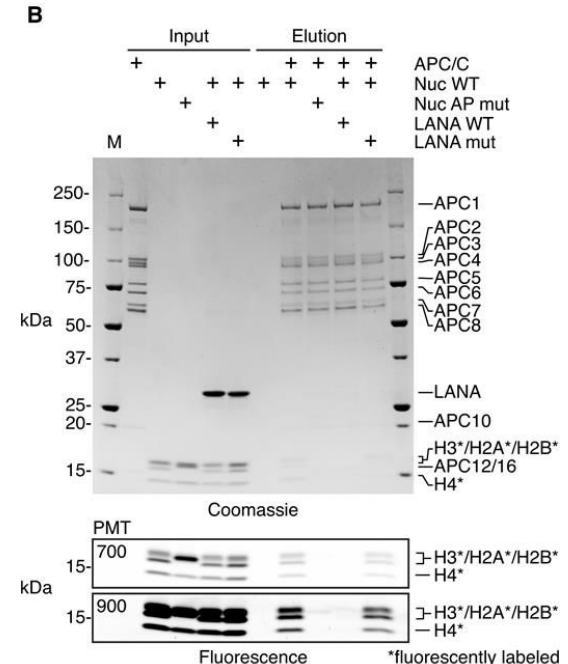
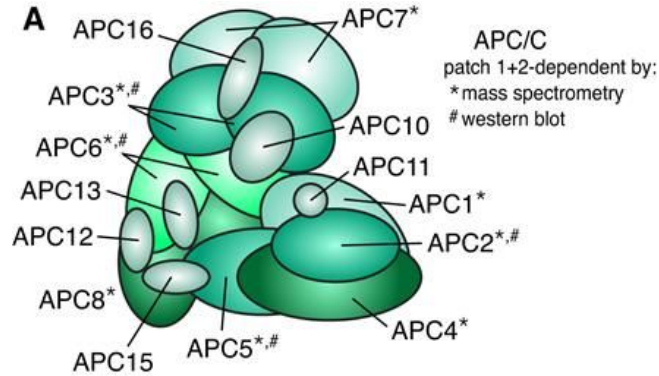
APC/C is a direct nucleosome acidic patch binder



Temporal pattern of APCCdc20 and APCCdh1 regulation throughout the cell cycle. During G1 phase of the cell cycle, APCCdh1 is an active complex. Once G1-cyclins accumulate, Cdh1 becomes phosphorylated and dissociates from the APC. This phosphorylation will be maintained until anaphase. From G2 to prophase, free APC is kept inactive by its inhibitor Emi1, which associates with Cdc20 and prevents APC-Cdc20 binding. At late prophase, Emi1 is degraded and RASSFA1 takes over the role of this inhibitor until late prometaphase when the latter is also proteolysed. Free APC is then phosphorylated by cyclin B/cdk1 and Plk1 kinases. At metaphase, APCCdc20 is still maintained inactive through direct binding of the checkpoint complex Mad2-Bub3-BubR1 (except for cyclin A and Nek2 proteolysis). Once the spindle checkpoint is satisfied, the Mad2-Bub3-BubR1 complex is dissociated from APCCdc20 and this ubiquitin-ligase achieves its full activity, and induces degradation of securin and initiation of cyclin B proteolysis. Continuous cyclin B degradation present during anaphase will ensure a decrease in cyclin B/cdk1 activity and a dephosphorylation of Cdh1, which in turn, will induce activation of APCCdh1 and degradation of Cdc20



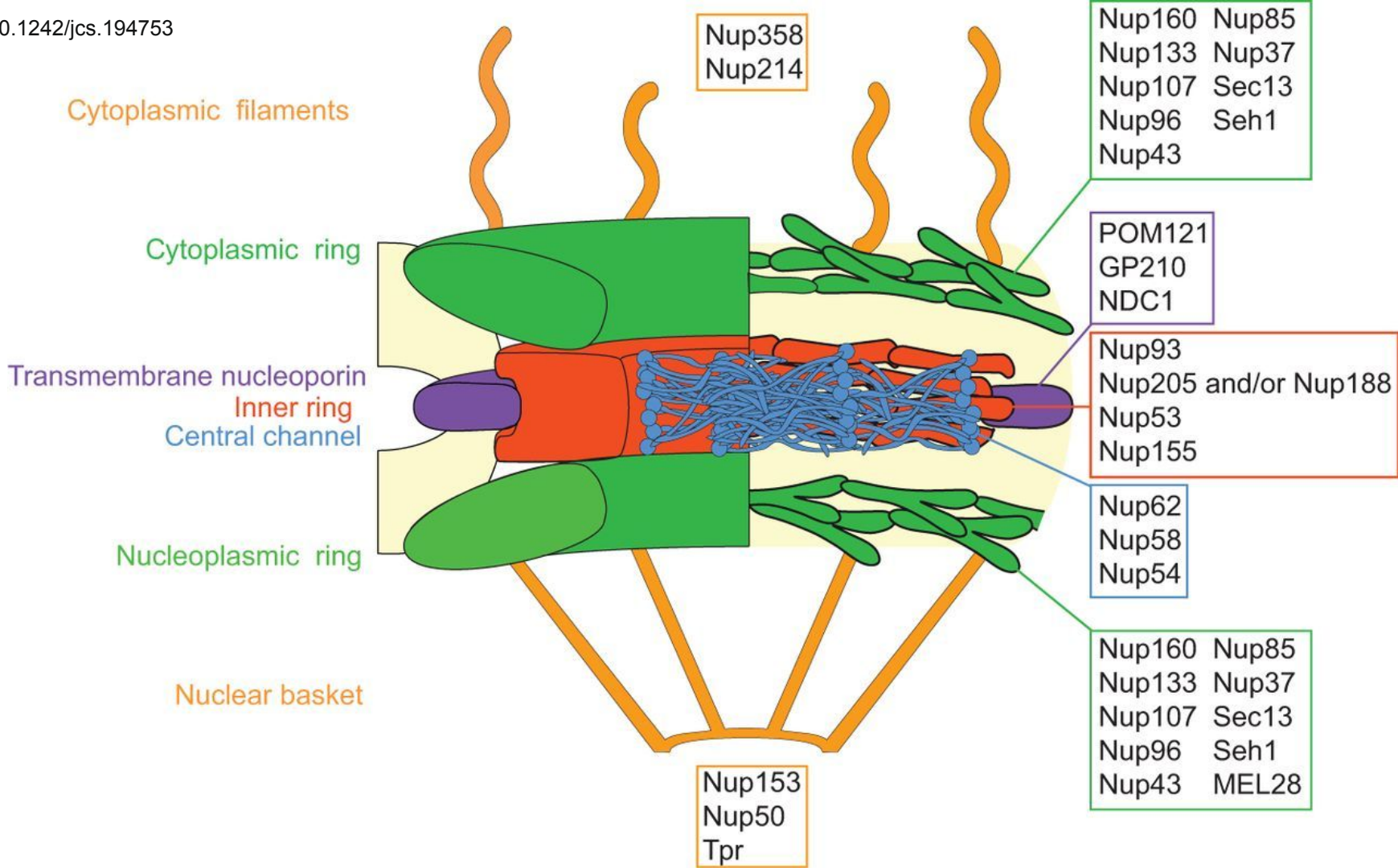
APC/C interacts directly with the nucleosome acidic patch



(A) APC/C composition with proteins identified to be patch 1- and 2-dependent by mass spectrometry and/or western blot indicated.

(B) Pull-down of WT or acidic patch mutant (AP mut) nucleosomes using immobilized recombinant twin-Strep-tagged APC/C alone or with WT or nucleosome binding deficient mutant of LANA (LANA mut). Histones are labeled with carboxyrhodamine (*) to facilitate high sensitivity detection by fluorescence imaging. Coomassie stained (top) and fluorescent images (bottom) of the same gel are shown. For fluorescent images, two different photomultiplier tube (PMT) settings were used for imaging (700 and 900). A PMT setting of 700 results in minimal pixel saturation. Imaging at a PMT setting of 900, which results in significant pixel saturation in input samples, increases sensitivity of elution samples to demonstrate minimal nucleosome binding in NCP AP mut and LANA WT elutions

ELYS binds to the nucleosome acidic patch with redundant basic sequences.



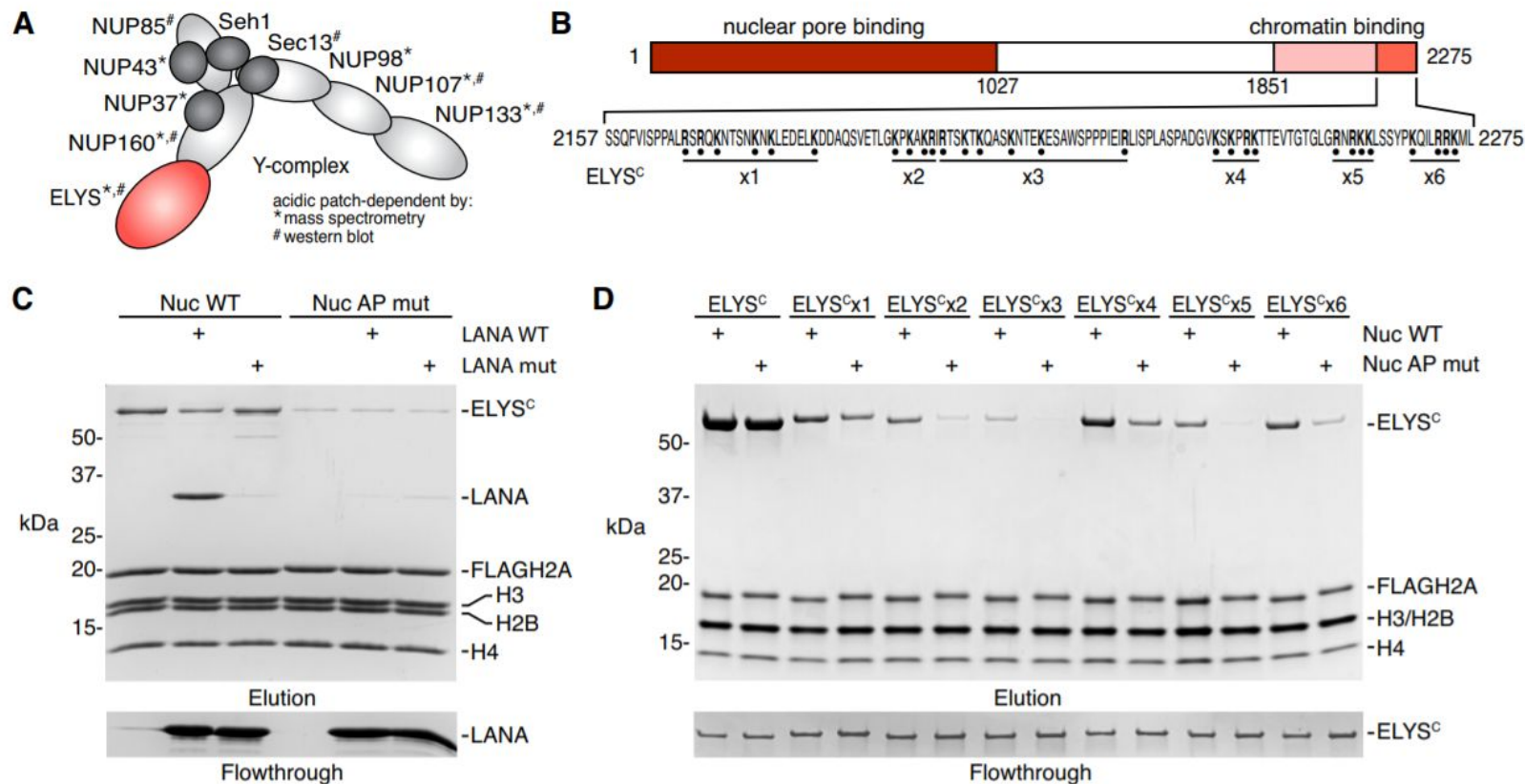
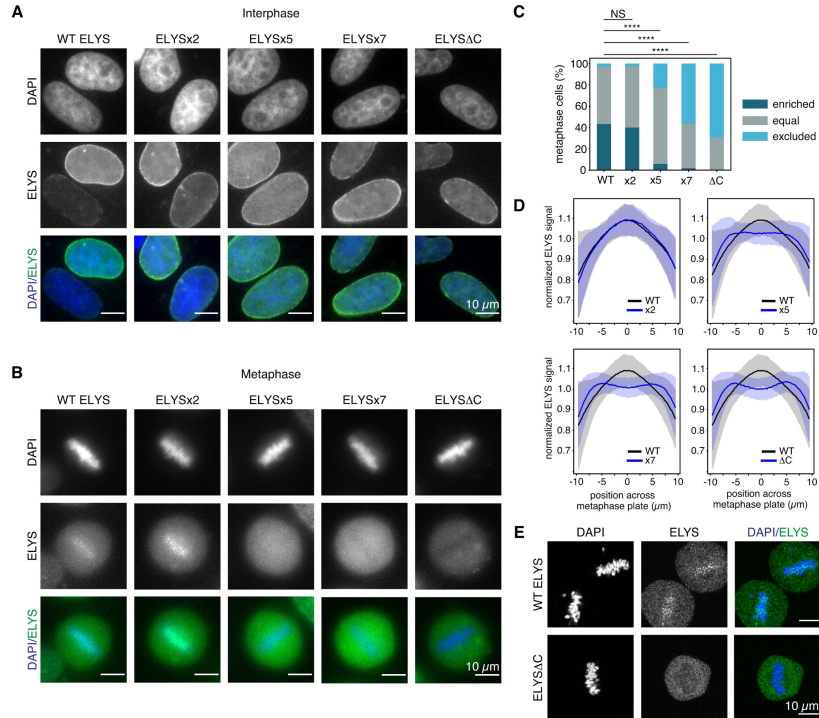


Figure 5. ELYS binds the acidic patch using redundant basic sequences. **(A)** Y-complex composition with proteins identified to be acidic patch-dependent by mass spectrometry and/or western blot indicated. **(B)** Schematic of ELYS indicating functional regions and ELYS^C sequence with Arg and Lys mutated to Ala in ELYS^Cx1-x6. **(C)** Pulldown of ELYS^C by WT or acidic patch mutant (AP mut) FLAG-tagged nucleosomes alone or with WT or nucleosome-binding deficient mutant of LANA (LANA mut) added as a competitor. **(D)** Pulldown of ELYS^C or ELYS^C mutants by WT and AP mut nucleosomes. Flowthrough in panels C and D demonstrate equivalent loading of ELYS or LANA variants, respectively.

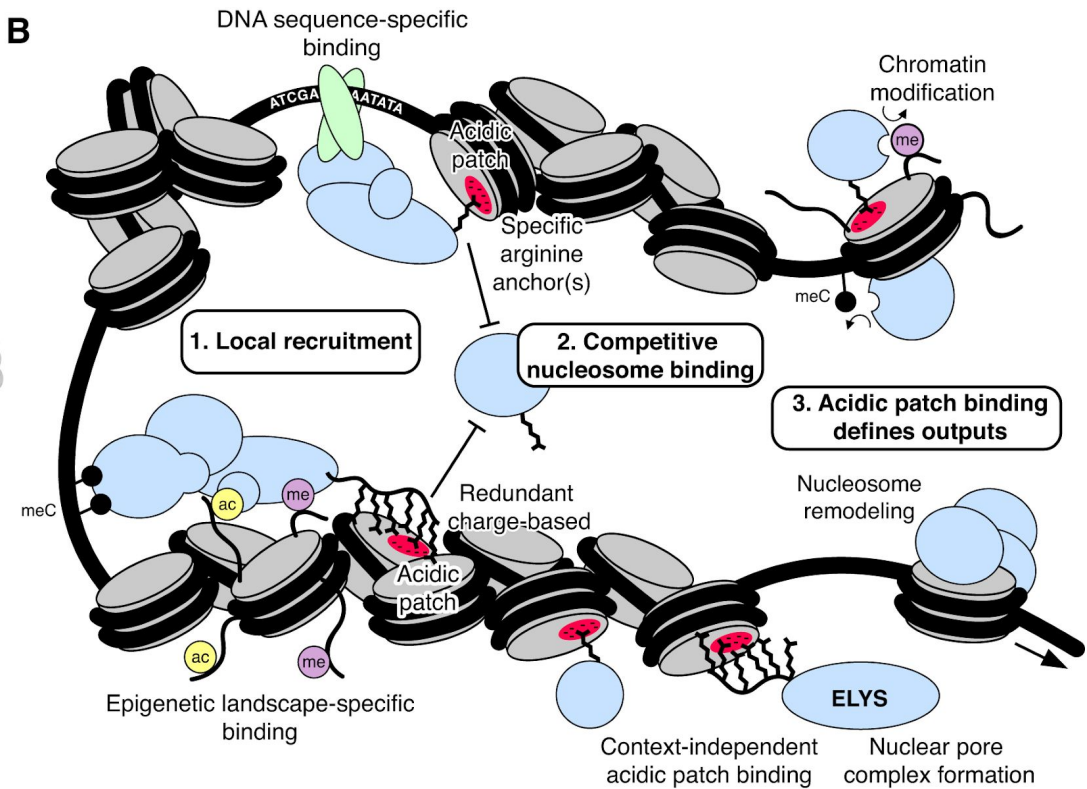
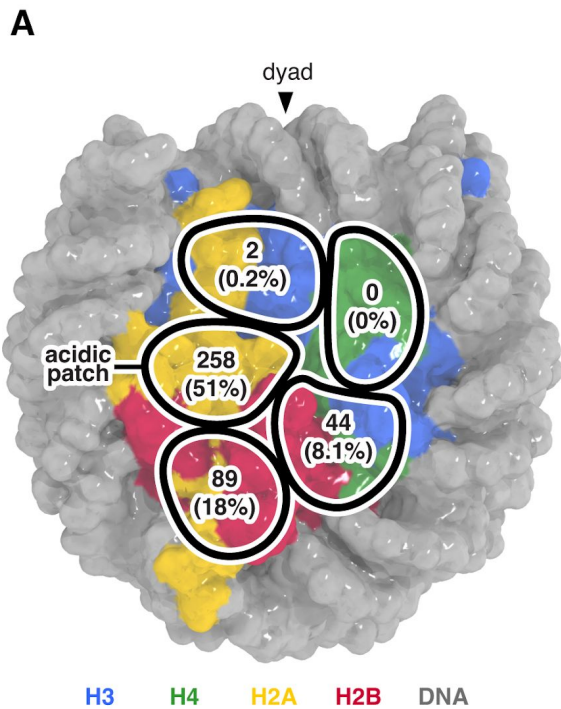
ELYS nucleosome binding regions are critical for metaphase plate localization.



ELYS requires redundant basic sequences for chromatin recruitment. **(A and B)** Interphase and metaphase images of HeLa cells expressing exogenous WT or mutant GFP-ELYS proteins. **(C)** Frequency of localization phenotypes, >100 cells scored for each GFP-ELYS variant. Statistical significance determined using Fisher's Exact Test with Bonferroni correction for multiple testing. (NS = not significant; **** indicates $P < 0.0001$). **(D)** Localization profiles of GFP-ELYS mutants across the metaphase plate for cells in panel (C). Line and shaded areas represent mean \pm 1 standard deviation. **(E)** Confocal images of metaphase cells.

DISCUSSION

- Acidic patch is the primary hot-spot for nucleosome binding that remarkably drives >50% of nucleosome interactions
- Two adjacent nucleosome patches mutated in Nuc2 and Nuc3 also contribute to nucleosome binding but almost entirely in an acidic patch-dependent context with larger impairments observed for the acidic patch mutant Nuc1 in nearly all cases.
- Nucleosome acidic patch binding commonly uses arginine anchors in both a canonical as well as variant locations



Nucleosome disk interaction hot-spots facilitate chromatin-templated processes. **(A)** Overview of nucleosome interactome screen results indicating number and percentage of identified proteins with decreased binding to nucleosomes containing mutations in each of the five nucleosome disk patches. **(B)** Schematic illustrating how competitive nucleosome disk binding combines with locus-specific chromatin recruitment to facilitate chromatin-templated processes.

DISCUSSION

- The canonical arginine anchor-binding cavity includes H2A residues E61, D90 and E92, two of which were mutated in Nuc1
- We suspect that some of the binding deficits in Nuc2 may actually reflect variant arginine anchors binding at the edge of the acidic patch in the vicinity of Nuc2 mutations of H2AQ24 and H2BQ47, E113 and K116.
- Nuc4, Nuc5 - comprise highly conserved H3 and H4 residues in region and may play specific roles in the nucleosome binding and function of a small subset of proteins (that have been previously implicated in transcriptional regulation in yeast)
- we observed large gains in protein binding to tailless nucleosomes, suggestive of more non-specific binding to nucleosomal and linker DNA that are typically shielded by the histone tails

Comparison with BioGRID

Of the 2142 histone interacting proteins in the BioGRID database, 485 were included in our dataset, accounting for **76%** of the proteins we identified and 23% of the BioGRID-identified histone interactors. As exemplified by APC/C and the Y-complex, our screen did not always identify every protein component of a nucleosome binding complex.

We find that **85%** of the proteins identified in our study are histone interactors or coexist in a complex (data from CORUM) with a histone interactor from the BioGRID database; conversely, **45%** of BioGRID histone interactors were either identified in our screen or coexist in a protein complex with a protein identified in our screen.

Unknown nucleosome binders

Demonstrated that one unexpected complex, the APC/C, binds directly to the nucleosome in an acidic patch-dependent manner

Elucidate a redundant mechanism of acidic patch binding by nuclear pore protein ELYS

